V. V. Sobolev[1],
orcid.org/0000-0003-1351-6674,
S. I. Gubenko[2],
orcid.org/0000-0001-6626-3979,
D. V. Rudakov[1],
orcid.org/0000-0001-7878-8692,
O. L. Kyrychenko[3],
orcid.org/0000-0002-1331-9323,
O. O. Balakin[3],
orcid.org/0000-0003-2003-0381

1 – Dnipro University of Technology, Dnipro, Ukraine, e-mail: velo1947@ukr.net
2 – National Metallurgical Academy of Ukraine, Dnipro, Ukraine
3 – State Enterprise "Research-Industrial Complex "Pavlohrad Chemical Plant", Pavlohrad, Dniproperovsk Region, Ukraine

INFLUENCE OF MECHANICAL AND THERMAL TREATMENTS ON MICROSTRUCTURAL TRANSFORMATIONS IN CAST IRONS AND PROPERTIES OF SYNTHESIZED DIAMOND CRYSTALS

Purpose. To analyze how the structural transformations in the cast iron metal matrix near graphite inclusions influence the features of synthesis of metastable diamond crystal on diamond polycrystals (substrate) synthesized by shock-waves.

Methodology. In experiments, we used the laser-induced detonation of explosive charges to create a flat shock-wave front and employed chemical, microstructural, spectral and X-ray phase analyzes. In particular, the features of chemical element distribution in cast iron phases, dislocation density in a solid solution, crystal lattice parameters, and others were studied.

Findings. It has been shown that solid-phase auto-epitaxy is a physically justified, experimentally proved and stably reproducible phenomenon. The accelerated transfer of carbon atoms to the surfaces of metastable diamond growing crystals in the kinetic mode is facilitated by a number of factors that cannot be quantified by numerically evaluated parameters. These include, first of all, the microstructure of the growing medium (cast iron matrix), carbon source, temperature and deformation fields that ensure transformation of polymorphic graphite to diamond with emerging gradient stress fields at the stages of forging, exposure to shock waves and thermal cycling. Defect redistribution in the crystal structure of the metal matrix and graphite inclusions plays a certain role at the mesoscale. It has been found that saturation with microstructural defects brings higher physicochemical activity to the system in the whole.

Originality. For the first time in world practice, diamond single crystals have been synthesized that contain the inclusions of polycrystalline diamond particles of shock-wave origin inside the single crystal shell; this may indicate a general discreteness of natural diamond formation.

Practical value. The growth of single metastable crystal on polycrystalline diamond of shock wave synthesis is the most favorable in case of using austenitic gray cast iron with foliate graphite inclusions. The experimentally proved diamond growth in a solid medium under pressure and temperature within the range of graphite stability can be used to develop new low-energy technologies for the synthesis of metastable diamond single crystals.

Keywords: *explosion, diamond, solid phase, auto-epitaxy, cast iron, physical fields*

Introduction. One of the most pressing problems in the field of diamond synthesis is the creation of low-energy-consuming methods for growing single crystals with specified physical, technical, chemical, functional, and other characteristics. In this context, studying the patterns of phase transitions and structural transformations occurring in a solid growth medium represented by cast irons as model alloys containing various carbon sources is the problems of fundamental interest.

The synthetic diamond era began in 1953 when B. Platen synthesized a diamond crystal in Sweden for the first time in the world. The following year, the experiments on synthetic diamond production were conducted in the United States. In the early 1960s, the technologies of industrial diamond synthesis were developed based on the advances in thermodynamics of mutual transition of graphite to diamond (O. I. Leipunsky, 1939) and the experiences of the reproducible method for diamond synthesis in Sweden, the USA and the USSR. The feature of the technology is the exposure of a mixture of graphite and metal catalyst powders to high pressures and high temperatures (HPHT). The specifics of this method are a short synthesis time ranging from several seconds to several hours needed for single crystal growth, while the pressure and temperature in the high-pressure chamber remain constant [1], whereby this synthesis is sometimes called the static method.

DeCarli F. S. and Jamieson J. L (1961) showed the fundamental possibility to synthesize diamond under microsecond exposure of graphite to strong shock waves. Over the last 25 years of the twentieth century the studies were focusing on the detonation synthesis of diamond as a superhard material [2]; recent studies explored the impact-wave synthesis by high-energy lasers using dense modifications of boron nitride [3].

Polycrystalline detonation diamonds were shaped by ultrafine particles interlocked with each other [4, 5]. The diamonds synthesized by using explosion energy depending on the preparation method were called either detonation diamonds emerging from atomic carbon in the detonation products of explosives [6, 7] or explosion diamonds synthesized, for example, in metal alloys containing graphite [4]. These diamonds with unique physical and chemical properties [5, 8] were demanded primarily in high-tech applications of mechanical engineering, metal processing, tools and machines, medical industry, etc.

In parallel with the HPHT technology development [9], the studies covered two directions:

1) physicochemical synthesis of single diamond crystals and diamond films by chemical vapor deposition (CVD method by Eversol W. G. 1962, Brinkman G. A. 1964, Derjaguin B. V. 1968);

2) nanodiamond synthesis in detonation products of blasting explosives (Volkov K. V., Danilenko V. V. and Elin V. I. 1962) reported in the studies of the All-Union Research Institute of Technical Physics, Snezhinsk, USSR [10, 11].

Today the HPHT and CVD methods are widely used industrial technologies for synthetic diamond production.

There was an extremely interesting challenge in the "diamond problem" for several centuries that combined searching for the methods for synthesizing diamond crystals of a given mass and substantiation of the statement that the diamonds appeared as an exceptionally high-pressure mineral. The studies on fundamentally possible physical conditions of nanodiamonds formation in atomic carbon gas began 37 years ago [12, 13]. Since 1973 the research teams of Dnipropetrovsk Mining Institute (now Dnipro University of Technology) and the Institute of Superhard Materials of the National Academy of Sciences of Ukraine did a series of studies on further development of the diamond synthesis technology by explosion [2, 4, 5].

In this paper we present the results of some studies developing the idea of potential metastable diamond crystallization performed under conditions of thermodynamic metastability governed by the carbon diagram "pressure-temperature". It should be noted that the concept of high-pressure nature of the diamond origin was one of the grounds for either aggressive criticism or a neutral attitude towards the idea of metastable diamond growth. The analysis of studies on the internal structure of diamonds from the primary deposits of South Africa and Yakutia, placer diamonds of the Urals, Central and South Africa [14−16], the features of discrete diamond growth [17], including those found in meteorites [18], the role of fluid phases in diamond formation [19] and the specifics of organic-element compounds involved in endogenous processes [20] demonstrated the need for reviewing the concept of the diamond origin. On that basis a scenario was firstly proposed in [12, 13] to describe physical and chemical features of the stable nanoscale growth of diamond particles in an atomic carbon gas excited by UV light. The proposed model assumed that diamonds appeared in carbon clouds of the interstellar medium before the protosolar cloud began to form. The key assumptions of this hypothesis were later repeatedly proved experimentally, for example, in [21−23].

In nature, carbon occurs in the form of carbon phases that are polyenes and cumulene chains, nanotubes, fullerenes, graphene, graphane, graphyne, minerals (diamond, graphite, chaoite, lonsdaleite) as well in carbon-containing phases; however, the gas consisting of only atomic carbon does not exist under terrestrial conditions. These carbon properties cause certain problems for diamond synthesis in high-pressure chambers within the range of diamond thermodynamic stability with graphite as the source material for synthesis.

Any change in pressure or temperature in the growing process is well known to result in a halt of the growth and appearance of new crystallization centers − diamond nuclei − in conformity with the changing degree of supersaturation or su-

percooling [24]. Such difficulties are common for diamond synthesis in the range of thermodynamic stability [25]. In 1939 O. I. Leipunsky proposed a theoretic solution to the problem of diamond synthesis from graphite by indicating threshold temperatures and pressures that meet the range of diamond thermodynamic stability above the line "graphite-diamond" in the carbon equilibrium diagram. In this case, diamond synthesis becomes, in principle, possible in presence of a metal as a carbon solvent. Reaching the given supersaturation with atomic carbon due to graphite dissolution in a molten metal is necessary for crystallization of the diamond with specified physical and mechanical properties.

Development of the technology for dynamic synthesis of superhard materials [2, 26, 27], the analysis of studies on metastable diamond growth (E. O. Mindeli, E. Sh. Chagelishvili, N. S. Turmanidze et al., 1979−1983; V. S. Kravtsov, L. G. Gankevich, 1986; A. R. Patel, K. A. Cherian, 1984) [28] and the experimental results obtained in our works [29, 30] originated the studies on the possibility of growing single crystals on polycrystalline diamonds generated by explosion. These studies covered the influence of the initial solid medium on diamond output [31], various thermal cycling conditions of cast iron after shock wave (SW) treatment [32], plastic strains followed by SW treatment [33], SW treatment followed by plastic strains [34, 35]. The physical properties of diamond crystals with the nuclei synthesized in a high-pressure chamber by the HPHT method and then grown under atmospheric pressure with passing a weak electric current through a technological mixture of a catalyst metal with graphite were studied in [36]. The methods for synthesis of metastable diamond using carbon nanophases as a source material were developed in [37].

The studies [31−35] gave some examples of the methods used for synthesis of metastable single crystals on polycrystalline explosion diamonds. The characteristic features of these methods are subsequent treatments; the primary treatment includes exposure to shock waves and plastic deformation whereas the secondary treatment does thermal cycling, plastic deformation, and passing a weak electric current.

In spite of the abovementioned advances, a number of phenomena remain practically undiscovered including the influence of mesoscale processes occurring in a carbon-containing medium under initial impacts and the influences of these processes on localizing of relaxation microstructural transformations near graphite inclusions, as well as appearance and growth of polycrystalline explosion diamonds.

This study aims to analyze the structural rearrangement effects that occur at the mesoscale level in the metal matrix of cast iron near graphite inclusions under the complex influence of physical fields on the properties of metastable crystals grown on diamond substrate by detonation synthesis.

Materials and methods. In the experiments, we used gray cast iron with foliated and spherical graphite (Table 1). The cast iron cylindrical samples of diameter 30 mm and height 9 mm were placed in a holder made of steel 40.

SW compression was generated using a metal plate accelerated by detonation products in the slit of width h as shown in Fig. 1, b.

Table 1

Chemical composition of cast iron

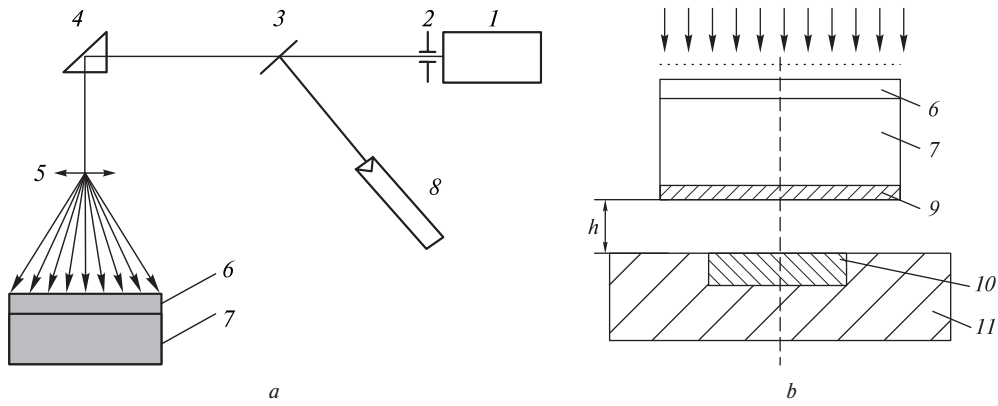| Nr.	Cast iron type	Concentration of elements, %					
		C	Mn	Si	S	P	Ni
1	Ferrite + foliate graphite	3.75	0.22	4	0.04	0.04	0.23
2	Austenite + foliate graphite	4	1.18	−	0.03	0.05	12.2
3	Austenite + spherical graphite	4	1.18	0.4	0.03	0.02	12.7

Fig. 1. Scheme of processing metal alloys by flat shock waves. Experimental setup for laser initiation of a photosensitive explosive (a) and device for diamond synthesis in cast iron by flat shock waves (b). Notations: optical quantum generator (laser) (1), aperture (2), glass plate (3), optical prism (4), scattering lens (5), the layer of a photosensitive explosive BC-2 (6), explosive charge of TNT/ RDX 40 alloy (7), calorimeter (8), metal plate-drummer (9), cast iron sample (10), steel clip (11). Arrows show laser emission

In practice, the slit width exceeded the plate thickness by 5−6 times. In this way, the maximum pressure in cast iron samples was achieved due to maximization of the plate acceleration velocity v. Within the specified slit the plate relative velocity v/v_D, where v_D is the velocity of explosive charge detonation, reached 0.45.

Explosive charges were made of TNT/RDX 40 alloy with the detonation velocity of about 7800 m/s. A laser-induced flat detonation wave in explosive charge 7 was followed by explosion of the initiating layer that contained BC-2 light-sensitive composite 6 with a mass density of 300 mg/cm^2 and a coating thickness about 2 mm (Fig. 1, b) [38−40]. A flat detonation front formed by explosive charge 7 accelerated striking metal plate 9. A neodymium solid-state optical quantum generator in glass 1 operating in the quality factor generation mode was used as the radiation source. The laser pulse duration was 30 ns, the pulse

energy 100 mJ, the radiation wavelength 1.06 μm; the laser beam was limited by aperture 2. A part of the radiation was deviated by glass plate 3 to measure the laser pulse energy in calorimeter 8. Prism 4 ensured laser beam rotation in the direction to a sample, and scattering lens 5 expanded the beam so that its diameter on the surface of BC-2 composite 6 reached 45 mm. The samples of cast iron 10 were cylinders of 5 mm high, 30 mm diameter placed in steel holder 11. The calculated heating temperatures of the iron matrix T_m and graphite inclusions T_g in the range from 50 GPa to 90 GPa were $T_m = 400$ K and $T_g = 770$ K at a pressure of 50 GPa; $T_m = 720$ K and $T_g = 1420$ K at a pressure of 90 GPa.

Results. *Cast iron microstructure features.* Plastic displacements and micro-rotations of the crystal lattice in the cast iron matrix, i.e. plastic strains of the matrix occur under SW treatment by sliding and vortex flow localized near graphite inclusions (Figs. 2, $a−d$). Along with that, the dislocation density
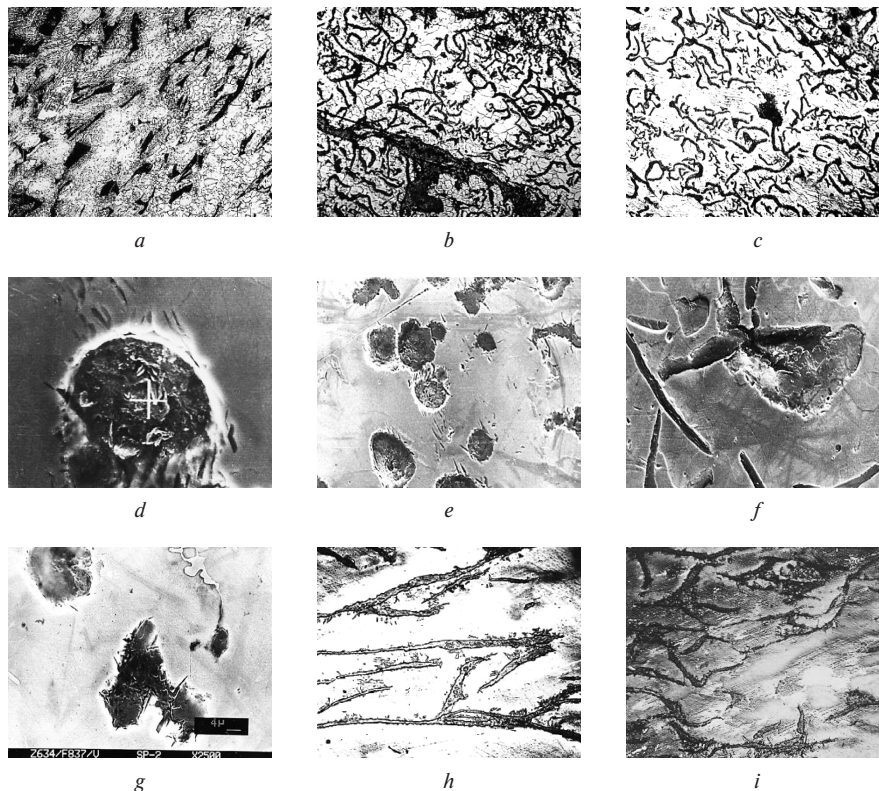

Fig. 2. Structure of cast iron 1 (a−c, g), cast iron 2 (f, h−i) and cast iron 3 (d, e) after SW treatment (a−g, i) and forging (h, i). Magnifications:
a−c − ×300; d, e − ×1000; f, g − ×2500; h, i − ′400

increases from $\sim 10^{-8}$ cm^{-2} in the initial as-cast condition to $(1.48 - 7.2) \cdot 10^{12}$ cm^{-2} after SW treatment. The microdistortion magnitude in the cast iron lattice significantly increased.

It should be noted that a non-conservative shifting of dislocation thresholds developed during the high-speed dislocation movement causes a large number of single defects. The temperature field generated by the thermal energy of adiabatic compression is unlikely to be homogeneous in cast iron samples because of the difference in the graphite and the metal matrix wave impedance. As a result, graphite inclusions are heated to the temperature higher than the matrix temperature, which affects their behavior under pulsed loading. The traces of plastic shifts were found in graphite (Fig. 2, *e*); a part of graphite inclusions underwent brittle destruction after shock compression (Figs. 2, *f, g*). Some of the samples were forged before SW treatment; as a result, graphite inclusions and liquation zones in the matrix were oriented perpendicularly to the impact direction (Figs. 2, *h, i*). Liquation phenomena were apparent in all examined elements as a result of abnormal mass transfer, which contributed to graphite transformation.

Localizing of plastic strains near graphite inclusions caused stresses and local strengthening the cast iron matrix. The microhardness in ferritic iron 1 was 1810 MPa far from inclusions; it increased to 2050 MPa at a plane boundary with a graphite inclusion and reached 2190 MPa at the inclusion ends; in austenitic iron 2 these values increased to 2030 MPa, 2200 MPa, and 2310 MPa, respectively.

During the mechanical treatment by SW and forging, a mesoscopic substructure is developing in the deformed cast iron, which relates to the appearance of localized strain mesostrips in various grains of the metal matrix along the maximum tangential stress directions [41]. Loading any hetero-phase material such as cast iron with graphite inclusions causes a sharply inhomogeneous distribution of stresses and strains; long-range momentum and asymmetric stresses arise due to the interactions between the metal matrix and graphite inclusions. This implies appearance of a tensor-spin field in vortex motion related to the stress-momentum tensor. The share of energy dissipation in vertex motion of a graphite inclusion makes several per cent of the visco-plastic flow energy dissipation in the matrix near the inclusion [41]. The stresses in a cast iron matrix relaxing with developing strains are transferred to graphite inclusions; as a result, the areas with relaxed momentum stresses or zones of vortex flow arise in the cast iron matrix (Fig. 3, *a*).

High-speed plastic strains under pulsed loading is well known to cause the appearance of clusters in metals, a cellular or fragmented substructure that contains split dislocations and grain boundaries, stacking faults, irregular and loop-shaped sub-boundaries, zones of the pre-twin state, micro-twins and others that lead to strong disorientation. These properties indicate a significant rotational component of plastic strains. The variety of relaxation processes occurring in the metal during SW treatment is due to the crystal lattice type of a metal or alloy and different energy of stacking fault that is low in FCC metals; for this reason, twinning and stacking faults are developing easier than in BCC metals.

Obviously, the patterns of structural changes caused by pulsed loading in the ferrite matrix of cast iron 1 and a BCC lattice are similar as well as in the austenitic matrix of cast iron 2 and 3 and a FCC lattice. These patterns relate to emerging complex structures, which evidence relaxation followed by local plastic strains. A common feature of relaxation processes is the occurrence of noticeable plastic shifts and rotations peculiar to a highly deformed state, when collective forms of motion arise in strongly interacting dislocation ensembles. Moreover, in the areas covered by a fragmented or cellular structure, large-scale heterogeneities of crystallographic orientation appear causing significant disorientations. Non-equilibrium structures with a high-charge density of dislocations appear.

The differences in the nature of relaxation phenomena in the cast iron matrix are mainly due to the crystal lattice type, which predetermines different energy of stacking faults and different behavior of twinning dislocations in BCC and FCC materials. As a result, twinning and emerging stacking faults considerably differ in the cast iron matrix 1 and cast iron 2 and 3; in particular, pre-twin state of the BCC material and appearance of a new ε-martensite phase in the FCC material. The difference is also apparent due to the behavior of dislocations and grain boundaries, such as their anomalous splitting in BCC materials and regular splitting in FCC materials.

Structural transformation in cast iron. SW treatment leads to emerging complex microstructures due to high-speed deformations and phase transformations. The metal grain structure is rearranged not only due to the elongation of grains affected by the "cold" explosion effect. The presence of vortex zones indicates the development of rotational strains that affects a significant number of cast iron matrix grains. More often, vortex strain zones appeared near graphite inclusions with turbulence zones; this contributed to vortex displacement or twisting the location pattern of deformed grains.

In addition to plastic flow localization in the zones of constrained strains near graphite inclusions, sliding appears along the graphite-matrix boundaries (Fig. 3, *b*) accompanied by
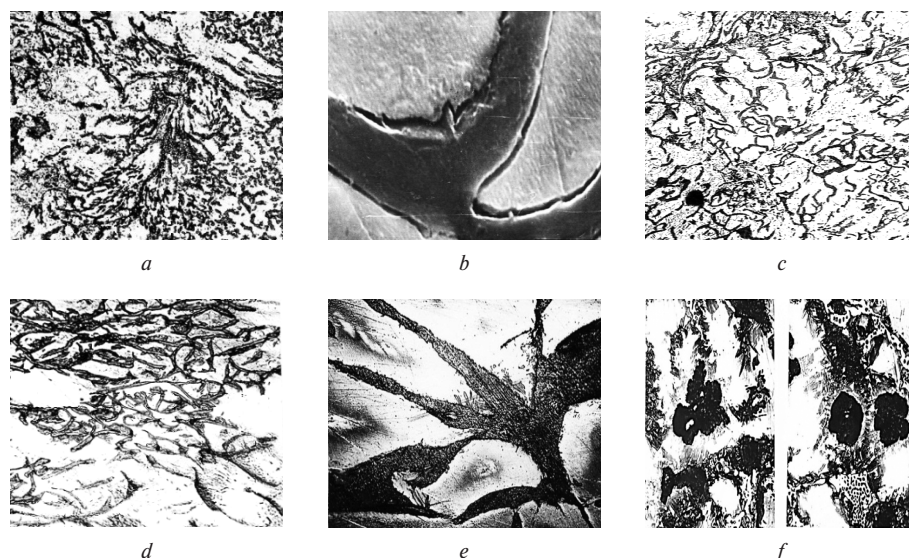

a   *b*   *c*

d   *e*   *f*

Fig. 3. Relaxation zones of stress strains near graphite inclusions. Magnification of ×400 (a, c, d), ×2500 (b), ×800 (e, f)

emerging periodic accommodation shifts near graphite. Such behavior of "graphite – matrix" boundaries, in contrast to high-temperature slipping refers to the cluster mechanism of mass transport with a "checkerboard" distribution of tensile and compressive stresses and strains. Mesostrips with localized strains appear near graphite inclusions that spread into grains along the directions of maximum tangential stresses (Figs. 3, *c, d*), which facilitates forming a mesoscopic substructure in the cast iron matrix. In addition, stress relaxation near graphite particles may occur due to local martensitic shifts (Fig. 2, *h*, Figs. 3, *e, f*), which, as known, is one of plastic strains mechanisms. Obviously, this is ε-martensite commonly growing in iron alloys under pulsed loading.

SW treatment intensifies boundary diffusion due to defective structure rearrangements within the "graphite – matrix" boundaries. This accelerates diffusion significantly contributing to graphite conversion into a diamond under thermal cycling. Complex rearrangements of boundary defects and impurities under loading may lead to evolving in time distribution of impurities both on the "graphite-matrix" boundary and in the cast iron matrix near the graphite inclusions. The appearing concentration gradient causes osmotic pressure related to the transition of various element atoms from the phase boundary to the matrix or to graphite inclusions. Therefore, graphite inclusions and phase boundaries "graphite – matrix" play an important functional role in nucleation of strain defects as a result of the cast iron treatment, thus influencing nucleation and growth of diamond inclusions.

X-ray microanalysis showed that graphite inclusions in the initial as-cast condition are chemically heterogeneous and contain a certain amount of impurities including 3.4 % Si and 4.1 % Mn in cast iron 1; 2.4 % Mn and 6.3 % Cr in cast iron 2; 7.6 % Si, 5 % Cr, and 6 % Mn in cast iron 3. SW treatment and forging lead to element redistribution in the cast iron matrix compared to the as-cast conditions, with growing crystals of various minerals as non-metallic inclusions, for example, eulite, moissanite, almandine, biotite, quartz, and so on. They were found mainly on phase and grain boundaries, whilst quartz particles – in micro- and macro-pores. New phases in the form of nonmetallic inclusions appear in a relatively short time of exposure to shock waves due to the excited state of atoms of various elements under high pressures and temperatures. Presumably, a multicomponent system with favorable proportions among chemical elements is developing in local microregions due to liquation.

Diamonds in cast iron microstructure. Polycrystalline diamonds that consist of multiple nanoscale single crystals were found in graphite inclusions after SW treatment of cast iron (Figs. 4, *a, b*). The assessed features for phase transformations of some graphite inclusions into diamonds are similar to those assessed in one of the first relevant studies (Trueb L. F., 1968).

Graphite conversion into a diamond is assumed to occur in a shear way due to short duration of SW treatment, which eliminates or minimizes diffusion movement of carbon atoms and impurities. Shear displacement is resulted by compressive and shear lattice strains accompanied by atom movements shorter than interatomic distances. Obviously, anomalous acceleration of mass transfer (Strong Y. V., Cherenko R. M., 1971) and long-range gradient stress fields contribute to graphite conversion into a diamond.

Diamonds do not grow in all types of graphite inclusions. In the case of foliated graphite, diamonds appear mainly in the inclusions oriented perpendicularly to the direction of SW front propagation. Therefore, to increase the diamond output it is necessary to orient the graphite in a certain direction. In the experiments, cast iron samples were forged in the way to turn them perpendicular to the acting pressure before SW treatment (Figs. 2, *h, i*). The share of rhombohedral graphite was found to increase from 6–7.5 % in the initial state to 50–60 % after plastic strains by forging depending on the cast iron type. Hexagonal graphite is known to convert to rhombohedral
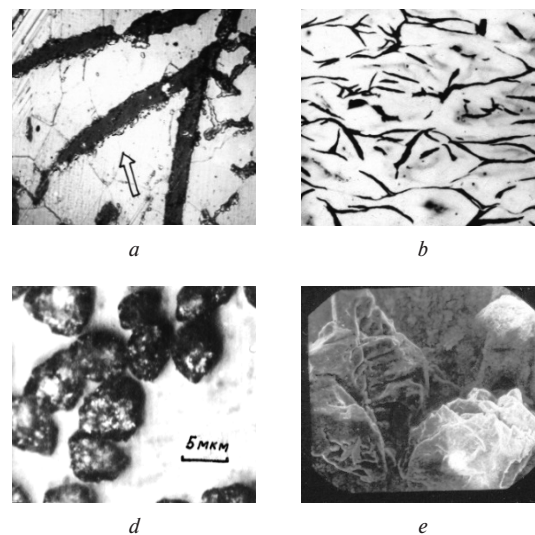

Fig. 4. Diamonds in the cast iron structure after SW treatment (a, c) and forging with SW treatment (b, d). Magnification of ×200×4 (a), ×500 (b), shown in picture (c), ×125×4 (d)

graphite by the shear mechanism as a result shifting the atomic layer in the lattice (Kurdyumov A. V., Piliankevich A. N., 1979).

The particle size of polycrystalline diamond appeared as a result of SW treatment ranged from 1 to 3 μm in the main fraction with the maximum yield of about 32 %, with a certain number of particles reaching the size of 10 μm. The largest particles of up to 200 μm size were found in pre-forged cast iron samples. Small mosaic blocks of ~140 Å and high dislocation density reaching ~10^{12} cm^{-2} are known to occur in diamond inclusions. This coincides with the results of the present study on evaluation of a dislocation density in cast iron samples after SW treatment. Diamond particles are polycrystalline aggregates with highly-developed non-singular surface (Figs. 4, *c, d*) that have a large number of areas potentially capable to grow rapidly.

The diamonds synthesized in cast iron by explosion are polycrystalline particles that consist of single crystals of mostly nano-sized range [41]. Additional thermal cycling after SW treatment of cast iron leads to appearance of single crystals (Fig. 5). In general, the mechanism of single crystal growth on polycrystalline diamond particles to a micro-size can be described as follows.

Alternating heating and cooling of a ferrite or austenitic matrix of cast iron cause intensive movement and defects redistribution in crystals, which accelerates diffusion of carbon atoms and impurities and overgrowth of a single crystal film on diamond seed particles. SW treatment activates the cast iron matrix by introducing a large number of crystal structure defects and contributes to increasing the carbon diffusion rate in the matrix when passing the SW front up to $10^{-2}–10^{-3}$ cm^2/s, whereas subsequent forging and thermal cycling intensify diffusion only to $10^{-5}–10^{-6}$ cm^2/s. These results were obtained by
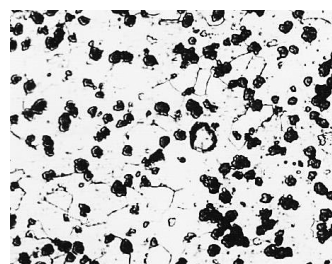

Fig. 5. Diamonds in the cast iron structure synthesized by SW treatment and thermal cycling. Magnification of ×1000

penetration depth evaluation for carbon from cast iron into a steel holder taking into account treatment duration [29–35]. Metal-physical studies of the contact "cast iron — steel" have revealed the largest diffusion changes when using austenitic cast iron 2 with foliated graphite.

The diamond crystals may grow both in kinetic and diffusion modes. In the studies [29–35] the correlations governing the crystal growth rates for various modes were evaluated for the given conditions of steady-state growth and when diffusion fluxes to different growth centers do not cross each other. A comparison of the diamond and graphite crystal growth rates in the system "graphite — solid carbon solution in iron — diamond" showed that the preferred diamond crystals growth (α) with respect to graphite growth (β) during the decomposition of a supersaturated solid carbon solution in a metal is possible only in the kinetic mode under the condition

$$(a_1\sigma_1)\alpha^2 < (a_2\sigma_2)\beta^2, \qquad (1)$$

where a_1 and a_2 are average distances between carbon atoms in the diamond and graphite lattices; σ_1 and σ_2 are the interfacial surface energy at the diamond and graphite solid solution boundary.

With a stress gradient, the concentration gradient of vacancies and, therefore, of "vacancy–carbon atom" complexes appear in the cast iron metal matrix, which enables their moving from the compressed zones of the lattice to stretched ones through grains or along grain boundaries. The velocity of such flows is governed by the diffusion rate on the grain boundary and the lattice. Under thermal cycling, stress is redistributed in long-range gradient fields.

The growth rate of diamond crystals is lower than the graphite growth rate in the diffusion mode because diamond growth is controlled by the carbon diffusion rate in the cast iron matrix so the chemical crystal properties of the competing phases do not have a significant effect. Thermodynamic factors prevail over kinetic ones; as a result, the appearance of a metastable phase slows down. A kinetic mode of diamond growth is possible only under high diffusion rate of carbon and vacancies, which is achieved by preliminary SW treatment. It generates a high density of linear and point defects in the cast iron matrix microstructure, thus contributing to the appearance of long-range gradient stress fields near graphite inclusions.

Thermal cycling provides the conditions for the preferred growth of metastable diamond with the dissolution of coarse graphite inclusions, the appearance of randomly distributed small graphite precipitations, as well as the dissolution of graphite that blocks the surface and passivates the subsequent diamond seed crystal growth. The passivating effect of graphite on diamond growth lies in the fact that graphite, as a more stable phase, cannot give carbon atoms to diamond directly through the phase boundary.

Carbon redistribution between the cast iron phases in one cycle (heating — suspending — cooling) can be described as follows. When heating, a certain amount of graphite and diamond dissolves and the solid solution is saturated with carbon. When cooling, the cast iron matrix is supersaturated with carbon and, as a result of decomposition of the solid solution, carbon atoms move into diamond and graphite as competing phases. Both carbon phases can grow; there is only a difference in the growth rate due to difference in the phase crystal chemical nature and the solid solution state.

To a first approximation, the molecular kinetic perception of the process can be described as follows. The increased vacancy concentration in the solid solution caused by SW treatment facilitates the accelerated evacuation of iron atoms and impurities from the interphase front "solid solution — high-carbon phase". However, in the case of diamond, the so-called normal growth occurs when each elementary act of iron atom removal is followed by carbon atom addition. This is the well-known catalytic effect of iron cubic packing on the growth of the diamond phase with the same packing.

In the case of graphite with its hexagonal layered structure, there is a tangential growth with the attachment of carbon atoms only if the vacancies are approaching the graphite lattice prismatic faces. Therefore, the increasing concentration potential of carbon influences predominantly the growth rate of diamond inclusions due to kinetic mode domination. Carbon solubility in the matrix of austenitic cast iron 2 and 3 decreases monotonously because of the absence of eutectoid transformation; this leads to continuous diamond particle growth. In contrast, carbon solubility in the matrix of cast iron 1 at the time of eutectoid transformation drops abruptly; as a result, the excess carbon is spent on nucleation of graphite as a stable phase, and less amount of carbon moves to diamond particles.

Subsequent treatment of gray cast iron by forging and SW, SW and thermal cycling allowed obtaining the diamond crystals fundamentally differing by their properties from the crystals grown during dynamic synthesis when using SW energy only and from the crystals synthesized in high-pressure chambers. Diamond particles are transparent, colorless, sometimes have different shades — yellow, green, less often blue and pink — that indicates the presence of impurities inherited from graphite during polymorphic transformation or captured from a solid solution during growth. The refraction index of the studied diamond particles of 2.4171 is close to the optical refraction index of natural diamonds. Growth forms of crystals vary in a wide range (Figs. 6, *a–h*) and include octahedron, rhombic dodecahedrons, and cubic octahedron. There are also drusen, aggregates of two or more crystals, skeletal crystals emerged as a result of the high growth rate inherent in the kinetic mode. The prominent vicinal surfaces often recognized on the faces evidence a dislocation growth mechanism (Figs. 6, *i–k*). The distinctive properties of diamond crystals grown in cast iron by the auto-epitaxial method are the appearance of rhombic dodecahedrons as well as blue, yellow-green and orange luminescence of crystals under UV light. The crystals grown in high-pressure chambers do not have these properties.

The Lauegrams of studied diamond particles (Fig. 6, *l*) enabled revealing the presence of a clearly defined polycrystalline seed, called a genetic center, in single crystals. This is a former explosion generated diamond particle having retained its physical properties such as high concentration of defects and polycrystalline structure due to interconnected nano-diamond particles. Table 2 demonstrates some specific features of synthesis of metastable single diamond crystals.

The physical specifics of single crystals grown on polycrystalline explosion diamonds are the presence of a genetic center, which indicates the discrete growth: it was experimentally proved internationally for the first time. The ability of growing diamond crystals to keep the genetic center and resume the once-started growth regardless of the pause duration is due to a decrease in supersaturation of the iron microstructure with carbon and the thermodynamic metastability conditions.

In this context, one can explain the genetic center presence in diamonds originated from primary deposits in Africa and Yakutia, and placer diamonds in the Urals, which was not unriddled for a long time. In the range of high pressures and high temperatures where diamond is thermodynamically stable, the discrete growth is impossible since any changes in supersaturation or supercooling in this range interrupt single crystal growth, with stimulating the appearance of new crystallization centers.

The structural feature of grown diamond crystals is the presence of two zones which are 1) a single crystal shell with a dislocation density of $(1.8–6.3) \cdot 10^{12}$ m^{-2} and 2) a polycrystalline center with a dislocation density of $10^{15}–10^{16}$ m^{-2}. The Lauegrams revealed a continuous diffuse ring on the background of single distinct diffraction maxima. Asterism is a consequence of the presence of a polycrystalline nucleus, which enhances the internal deformation of a single crystal. In this regard, we state that the crystals studied have a genetic center with rudimentary features of a dynamically derived nu-
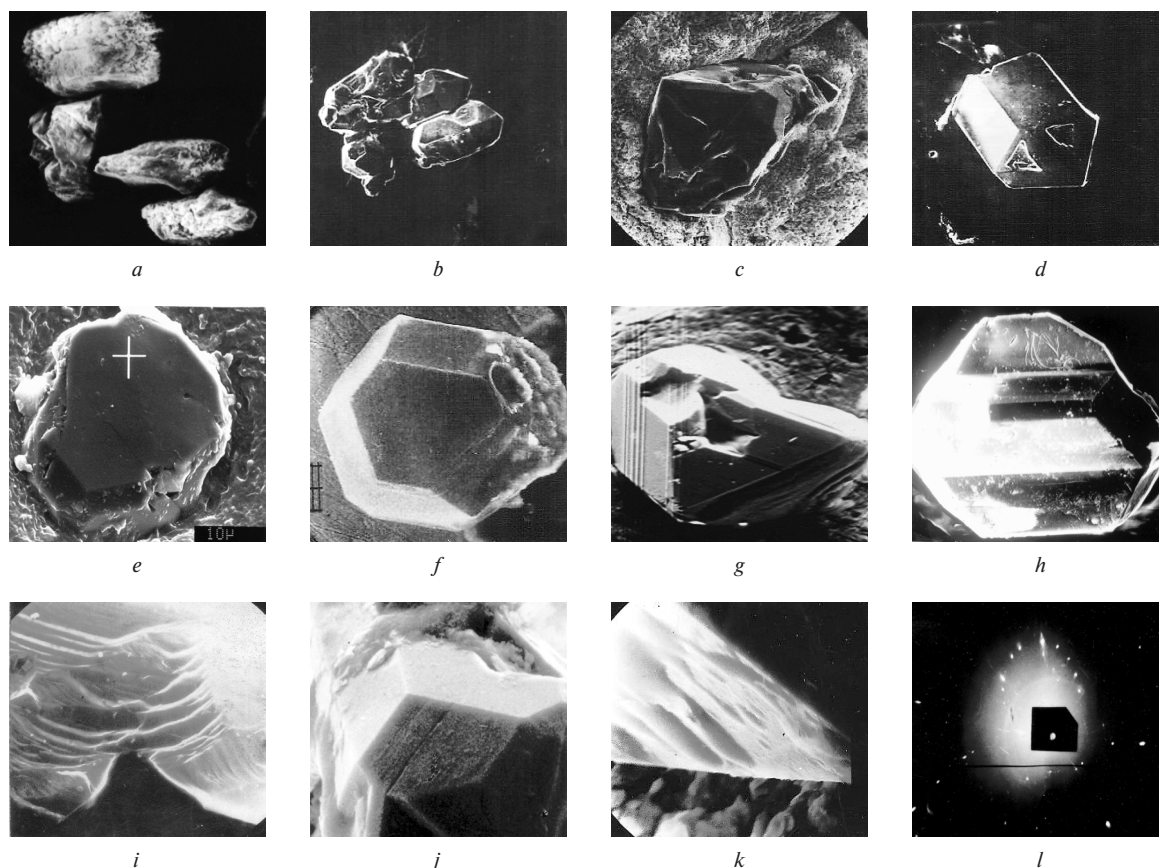
Fig. 6. Diamond crystals grown on cast iron after SW treatment (a), SW treatment and thermal cycling (c, i, k, j), forging and SW treatment (b, d, e,f, g, h); Lauegram of single diamond crystal (l). Magnification of ×1200(a), ×70 (b), ×400 (c), ×250 (d), ×1000 (e), ×250 (f), ×250 (g), ′800 (i), ×200 (j), ×200 (h), ×1000(k)

Table 2

Key physical features of diamond synthesized by the HTHP method and SW treatment (SWT) followed by the growth of single diamond crystals

Nr.	Synthesis parameters	Stage 1. Nucleation		Stage 2. Growth	
		SWT	HPHT	SWT	HPHT
1	Pressure, Pa	$> 2 \cdot 10^{10}$	$(4{-}10) \cdot 10^9$	$10^5{-}10^7$	$(4{-}10) \cdot 10^9$
2	Temperature, K	<3500	<2000	<1000	<2000
3	Nucleation conditions	Spontaneous	Spontaneous	n/a	n/a
4	Transition specifics from Stage 1 to Stage 2	Discrete, less commonly continuous			
		Continuous only			
5	Single crystal size, m	$10^{-9}{-}10^{-8}$	$10^{-9}{-}10^{-8}$	$10^{-5}{-}10^{-4}$	$10^{-5}{-}10^{-2}$
6	Type of synthesized particles	Polycrystalline	Single crystals	Single crystals, crystal-jams	Single crystals, crystal-jams
7	Presence of a genetic center in single crystals	No	No	Yes	No
8	Luminescence under UV light	No	No	Yes	No
9	Isotope fractioning of carbon	No	No	Yes	No

cleus, which must be taken into account when interpreting the conditions of diamond appearance in nature.

The main fraction of grown diamonds contained the particles of the size from 100 to 150 μm; larger particles reaching 400 μm were grown in austenitic cast iron 2. This can be explained by a non-equilibrium form of foliated graphite inclusions more prone to dissolution when heating, thus able to supply more carbon to the solid solution in comparison to spherical particles in cast iron 3, as well as with higher stress gradients in the cast iron matrix near foliated graphite in comparison to spherical graphite. In addition, the advan-

tages of cast iron 2 are related to the presence of an austenitic matrix in the initial state, in which carbon redistribution under thermal cycling develops more favorably in terms of diamond growth conditions than in cast iron 1 with the same graphite form.

The optimal number of cycles during thermal cycling ranged from 3 to 5. A further increase in the cycle number did not result in a crystal size increase. This can be explained by the attenuation of diffusion fluxes due to exhaustion of non-equilibrium vacancy reserves generated by SW treatment, as well as the stress relaxation and a gradient decrease in the sys-

tem of long-range stress fields near graphite inclusions arising due to SW treatment.

Therefore, diamond solid-state auto-epithaxy in a carbon-containing medium is the result of a favorable combination of several factors including the composition and structure of the growth medium (cast iron matrix), carbon source (graphite), temperature and deformation fields that ensure polymorphic conversion of graphite into a diamond, the appearance of gradient stress fields, as well as the redistribution of defects in the crystal structure at the mesoscale during the stages of forging, SW and thermal treatments, which contribute to the predominant diamond growth in the kinetic mode under thermodynamic metastability conditions.

Conclusions. SW treatment of cast irons leads to emerging dispersed polycrystalline diamond of size ranging from 1 μm to 3 μm with the maximum yield of about 32 %. Polycrystals with a highly developed surface are potentially capable of further growth during thermal cyclic processing of the cast iron microstructure. The dynamic synthesis diamond can continue to grow in the kinetic mode with further thermal cycling or forging. The chemical activity of the studied heterogeneous system is due to the influence of high concentration of defects in the microstructure of the cast iron matrix and graphite inclusions, which helps to accelerate the delivery of carbon atoms to growing diamond particles. The use of forging before SW treatment leads to the orientation of graphite inclusions perpendicular to the pressure direction and contributes to a significant increase in the explosion diamond output. The most stable and reproducible process for growing a single crystal shell on explosion diamonds is austenitic gray cast iron with foliated graphite.

Mechanical and thermal treatment of cast iron includes two most important stages, which, regardless of the application sequence are as follows: 1) appearance of microstructures in the iron matrix and graphite inclusions with a reserve of additional internal energy within the range of graphite thermodynamic stability; 2) creation of shock compression pressures for phase transition of graphite to diamond.

Single crystal shell grows on a polycrystalline diamond substrate mainly if the carbon was in a solid solution state and the iron microstructure has a certain energy reserve additionally obtained as a result of thermal and mechanical treatments.

The process of emerging of a single crystal shell on polycrystals does not correspond to a typical synthesis at high stable values of p and T parameters, which occurs as a continuous growth from nucleation to the end of crystal growth. However, there is no clear understanding up to now of the role of the sample temperature after shock compression, the kinetics of solid carbon solution decomposition during cast iron cooling; besides, there are no ideas about the details of solid-phase growth of single crystals in the range of thermodynamic metastability. Thus, one of the tasks of follow-up research is the study of these issues taking into account the available experimental data on matching the properties of synthesized and natural single crystals.

References.
1. D'Haenens-Johansson, U. F. S., Katrusha, A., Soe Moe, K., Johnson, P., & Wang, W. (2015). Large colorless HPHT-grown synthetic gem diamonds from new diamond technology, Russia. *Gems & Gemology*, *51*(3), 280-299.
2. Breusov, O. N., & Dremin, A. N. (2008). Dynamic synthesis of superhard materials. *Chemical physics*, *27*(4), 21-33.
3. Kraus, D., Ravasio, A., Gauthier, M., Gericke, D. O., Vorberger, J., Frydrych, S., Helfrich, J., ..., & Roth, M. (2016). Nanosecond formation of diamond and lonsdaleite by shock compression of graphite. *Nature Communications*, 7: 10970. https://doi.org/10.1038/ncomms10970.
4. Bakul', V. N., & Andreev, V. D. (1975). Diamonds of the AB brand synthesized by the explosion. *Synthetic diamonds*, *41*(5), 3-4.
5. Sozin, Yu. I., & Belyankina, A. V. (1976). The substructure of a diamond synthesized by an explosion. *Synthetic diamonds,* (5), 27-29.
6. Danilenko, V. V. (2003). *Synthesis and sintering of diamond by explosion*. Moscow: Energoatomizdat. ISBN 5-283-01280-8.
7. Popov, V. A. (2016). Examination of non-agglomerated nanodiamonds inside aluminum matrix composites by synchrotron radiation. In: Z. Bartul, & J. Trenor (Eds.) *Advacers in Nanotechnologies.* New York: Nova Science Publishers. (pp. 185-202).
8. Andreev, V. D., Lukash, V. A., Voloshin, M. N., & Vishnevsky, A. S. (1981). Structural and phase transformations of graphite in cast iron under dynamic loading and morphological characteristics of the diamonds formed. *Physics and technology of high pressure*, (6), 61-64.
9. Eaton-Magaña, S., Shigley, J. E., & Breeding, C. M. (2017). Observations on HPHT-grown synthetic diamonds: a review. *Gems & Gemology*, *53*(3), 262-284.
10. Dolmatov, V. Yu. (2003). *Ultrafine detonation synthesized diamonds: production, properties, application: monograph*. Saint Petersburg: Publishing house of SPb SPU.
11. Shugaley, I. V., Sudarikov, A. M., Voznyakovsky, A. P., Tselinsky, I. V., Garabadzhiu, A. V., & Ilyushin, M. A. (2012). *Surface chemistry of detonation nanodiamonds as the basis for the creation of biomedical products: monograph*. Saint Petersburg:Leningrad State University.
12. Sobolev, V. V. (1985). The hypothesis on diamond formation in nature and possible reasons for its wide distribution on Earth. *Detonation. Proc. III All-Union Conference on Detonation, Nov 11-14. 1985, Tallinn-Chernogolovka: OIHF AN USSR,* 174.
13. Sobolev, V. V. (1987). Diamond crystallization in nature. *Combustion, Explosion, and Shock Waves*, *23*(1), 83-86.
14. Posukhova, T. V., & Kolume, F. N. (2009). Diamonds from placers of West and Central Africa — a problem of primary sources. *Bulletin of Moscow University, Series 4. Geology,* (3), 36-45.
15. Logvinova, A. M., Zedgenizov, D. A., & Sobolev, N. V. (2013). Genetic interpretation of mineral crystal fluid inclusions in diamonds. *Mineralogy Journal*, *35*(2), 39-48.
16. Simakov, S. K., Dubinchuk, V. T., Novikov, M. P., & Melnik, N. N. (2010). Metastable nanosized diamond formation from fluid phase. *SRX Geosciences*, 1-6. https://doi.org/10.3814/2010/504243.
17. Garanin, V. K. (1990). To the problem of discreteness of natural diamond formation. *Mineralogical journal*, (5), 28-36.
18. Gillet, P., & El Goresy, A. (2013). Shock events in the solar system: the message from minerals in terrestrial planets and asteroids. *Annual Review of Earth Planetary Sciences, 41*, 257-285.
19. Nikolsky, N. S. (1987). *Fluid regime of endogenous mineral formation*. Moscow: Nauka.
20. Slobodskoy, R. M. (1981). *Organic element compounds in magmatogenic and ore-forming processes*. Novosibirsk: Nauka.
21. Lewis, R. S., Ming, T., Wacker, J. F., Anders, E., & Steel, E. (1987). Interstellar diamond in meteorites. *Nature, 326*, 160-162.
22. Bernatowicz, T., Fraundorf, G., Tang, M., Anders, E., Wopenka, B., Zinner, E., & Fraundorf, P. (1987). Evidence for interstellar SiC in the Murray carbonaceous meteorite. *Nature, 330*, 728-730.
23. Anders, E. (1991). Organic matter in meteorites and comets: possible origins. *Space Science Reviews*, *56*, 157-166.
24. Volmer, M. (1939). *Kinetik der Phasenbildung*. Verlag Th. Steinkopff, Dresden und Leipzig. https://doi.org/10.1002/ange.19390523006.
25. Bataleva, Yu., Palyanov, Yu., Borzdov, Yu., Novoselov, I., & Bayukov, O. (2018). Graphite and diamond formation in

the carbide-oxide-carbonate interactions (experimental modeling under mantle P,T-conditions). *Minerals, 522*(8), 19. https://doi.org/10.3390/min8110522.

26. Breusov, O. N. (2002). On the mechanism of dynamic synthesis of diamond from organic substances. *Khimicheskaya Fizika, 21*(11), 110-115.

27. Batsanov, S. S. (2006). Features of solid-phase transformations initiated by shock waves. *Uspekhi Khimii, 75*(7), 673-686.

28. Angus, J. C., & Hayman, C. C. (1988). Low-pressure, metastable growth of diamond and diamondlike phases. *Science, 241*, 913-921.

29. Sobolev, V. V., & Slobodskoy, V. Ya. (1985). Crystallization of super-hard phases from solid solution carbon. *Crystallography, 30*(6), 1213-1214.

30. Sobolev, V. V., Didyk, R. P., Slobodskoy, V. Ya., Merezhko, Yu. I., & Skidanenko, A. I. (1983). Dynamic effects in the production of diamond from solid-solution carbon. *Combustion, Explosion, and Shock Waves, 19*(5), 658-659. https://doi.org/10.1007/BF00750451.

31. Gubenko, S. I., Slobodskoy, V. Ya., Sobolev, V. V., & Udoev, A. A. (1989). Investigation of a medium for diamond crystallization. *Russian metallurgy. Metally,* (6), 173-175.

32. Taran, Yu. N., Sobolev, V. V., Slobodskoy, V. Ya., & Gubenko, S. I. (1991). Formation of diamond inclusions in grey iron at combination of shock-wave treatment and thermal cycling. *Izvestiya AN SSSR. Metally,* (3), 140-147.

33. Sobolev, V. V., Taran, Yu. N., & Gubenko, S. I. (1993). Synthesis of diamond in cast iron. *Metallovedenie i Termicheskaya Obrabotka Metallov,* (1), 2-6.

34. Sobolev, V. V., Taran, Y. N., & Gubenko, S. I. (1997). Shock wave use for diamond synthesis. *Journal De Physique. IV JP, 7*(3), C3-73–C3-75.

35. Sobolev, V. V., Merezhko, Yu. I., Taran, Yu. N., Gubenko, S. I., Kalinushkin, E. P., & Slobodskoy, V. Ya. (2005). The phenomenon of solid-phase auto-epitaxy of diamond under the combined effects of physical fields. *Teoriya i praktika metallurgii,* (1-2), 108-112.

36. Sobolev, V. V., & Bondarenko, E. V. (1993). The change in granulometric composition of diamond crystals when treating synthesis products in electromagnetic field. *Sverkhtverdye Materialy, 4*, 57-58.

37. Luo, C., Qi, X., Pan, C., & Yang, W. (2015). Diamond synthesis from carbon nanofibers at low temperature and low pressure. *Scientific Reports, 5*, 13879. https://doi.org/10.1038/srep13879.

38. Chernai, A. V., Sobolev, V. V., Ilyushin, M. A., & Zhitnik, N. E. (1994). The method for obtaining mechanical loading pulses based on a laser initiation of explosion of explosive coatings. *Fizika Goreniya i Vzryva, 30*(2), 106-111.

39. Chernai, A. V., Sobolev, V. V., Ilyushin, M. A., & Zhitnik, N. E. (1994). Generating mechanical pulses by the laser blasting of explosive coating. *Combustion, Explosion, and Shock Waves, 30*(2), 239-242. https://doi.org/10.1007/BF00786134.

40. Nalisko, M., Sobolev, V., Rudakov, D., & Bilan, N. (2019). Assessing safety conditions in underground excavations after a methane-air mixture explosion. *E3S Web of Conferences Ukrainian School of Mining Engineering, 123*, 01008. https://doi.org/10.1051/e3sconf/201912301008.

41. Gubenko, S. I. (2015). *Non-metallic inclusions and strength of steel*. Saarbrücken: LAP LAMBERT. Palmarium academic publishing.

Вплив механічних і термічних дій на мікроструктурні перетворення в чавуні та властивості синтезованих кристалів алмазу

В. В. Соболєв[1], *С. И. Губенко*[2], *Д. В. Рудаков*[1], *О. Л. Кириченко*[3], *О. О. Балакін*[3]

1 — Національний технічний університет «Дніпровська політехніка», м. Дніпро, Україна, e-mail: velo1947@ukr.net
2 — Національна металургійна академія України, м. Дніпро, Україна
3 — Державне підприємство «Науково-виробниче об'єднання «Павлоградський хімічний завод», м. Павлоград, Дніпропетровська обл., Україна

Мета. Аналіз впливу структурних перетворень у металевій матриці чавунів поблизу графітних включень на особливості синтезу монокристалів метастабільного алмаза на алмазних полікристалах (підкладках) ударно-хвильового синтезу.

Методика. При проведенні експериментальних робіт використовувалася методика лазерного збудження детонації в заряді вибухової речовини для створення плоского фронту детонації. Проводився хімічний, мікроструктурний, спектральний, рентгенофазовий аналіз чавунів. Зокрема, досліджувалися особливості розподілу хімічних елементів у фазах чавуну, щільність дислокацій у твердому розчині, параметри кристалічної решітки та ін.

Результати. Показано, що твердофазна автоепітаксія є фізично обґрунтованим, експериментально підтвердженим і стабільно відтвореним явищем. Прискореному переносу атомів вуглецю до поверхонь зростаючих кристалів метастабільного алмаза в кінетичному режимі сприяє низка факторів, значення яких не є чітко фіксованими величинами й характеристиками. Це перш за все склад, мікроструктура ростового середовища (матриця чавуну), джерело вуглецю; температура й деформаційні поля, що забезпечують проходження поліморфного перетворення графіту в алмаз і виникнення градієнтних полів напружень на стадіях кування, ударно-хвильової дії й термоциклювання. Певну роль на мезорівні виконують закономірності перерозподілу дефектів кристалічної будови металевої матриці та включень графіту. Встановлено, що насичення мікроструктурними дефектами надає системі в цілому відносно високу фізико-хімічну активність.

Наукова новизна. Уперше у світовій практиці синтезовані монокристали алмаза, що містять усередині монокристалічної оболонки включення полікристалічних алмазних частинок ударно-хвильового походження, що може свідчити в цілому про дискретність природного алмазоутворення.

Практична значимість. Зростання монокристалів метастабільного алмаза на полікристалах алмазу вибухового синтезу є найбільш сприятливим у разі використання аустенітного сірого чавуну із включеннями графіту пластинчастої форми. Експериментально встановлений ефект зростання алмазу у твердому середовищі при тиску й температурі, що відповідають області стабільності графіту, може бути використаний при розробці нових ненергоємних технологій синтезу метастабільних монокристалів алмазу.

Ключові слова: *вибух, алмаз, тверда фаза, автоепітаксія, чавун, фізичні поля*

Влияние механических и термических воздействий на микроструктурные превращения в чугунах и свойства синтезируемых кристаллов алмаза

В. В. Соболев[1], *С. И. Губенко*[2], *Д. В. Рудаков*[1], *А. Л. Кириченко*[3], *О. А. Балакин*[3]

1 — Национальный технический университет «Днепровская политехника», г. Днепр, Украина, e-mail: velo1947@ukr.net

2 – Национальная металлургическая академия Украины, г. Днепр, Украина

3 – Государственное предприятие «Научно-производственное объединение «Павлоградский химический завод», г. Павлоград, Днепропетровская обл., Украина

Цель. Анализ влияния структурных превращений в металлической матрице чугунов вблизи графитных включений на особенности синтеза монокристаллов метастабильного алмаза на алмазных поликристаллах (подложках) ударно-волнового синтеза.

Методика. При проведении экспериментальных работ использовалась методика лазерного возбуждения детонации в заряде взрывчатого вещества для создания плоского фронта детонации. Проводился химический, микроструктурный, спектральный, рентгенофазовый анализ чугунов. В частности, исследовались особенности распределения химических элементов в фазах чугуна, плотность дислокаций в твердом растворе, параметры кристаллической решетки и др.

Результаты. Показано, что твердофазная автоэпитаксия является физически обоснованным, экспериментально подтвержденным и устойчиво воспроизводимым явлением. Ускоренному переносу атомов углерода к поверхностям растущих кристаллов метастабильного алмаза в кинетическом режиме способствует ряд факторов, значения которых не являются строго фиксированными величинами и характеристиками. Это прежде всего состав, микроструктура ростовой среды (матрица чугуна), источник углерода; температура и деформационные поля, обеспечивающие прохождение полиморфного превращения графита в алмаз и возникновение градиентных полей напряжений на стадиях ковки, ударно-волнового воздействия и термоциклирования. Определенную роль на мезоуровне выполняют закономерности перераспределения дефектов кристаллического строения металлической матрицы и включений графита. Установлено, что насыщение микроструктурными дефектами придает системе в целом относительно высокую физико-химическую активность.

Научная новизна. Впервые в мировой практике синтезированы монокристаллы алмаза, содержащие внутри монокристальной оболочки включения поликристаллических алмазных частиц ударно-волнового происхождения, что может свидетельствовать в целом о дискретности природного алмазообразования.

Практическая значимость. Рост монокристаллов метастабильного алмаза на поликристаллах алмаза взрывного синтеза является наиболее благоприятным в случае использования аустенитного серого чугуна с включениями графита пластинчатой формы. Экспериментально установленный эффект роста алмаза в твердой среде при давлении и температуре, отвечающих области стабильности графита, может быть использован при разработке новых неэнергоемких технологий синтеза метастабильных монокристаллов алмаза.

Ключевые слова: *взрыв, алмаз, твердая фаза, автоэпитаксия, чугун, физические поля*